RSC Advances

PAPER

View Article Online
View Journal | View Issue

Cite this: *RSC Adv.*, 2020, **10**, 35949

AuNPs@PMo_{12} nanozyme: highly oxidase mimetic activity for sensitive and specific colorimetric detection of acetaminophen†

Tahereh Rohani Bastami *[a] and Zeynab Dabirifar[b]

The design of a highly specific and sensitive approach for the quantitative and qualitative determination of acetaminophen (AP) is crucial from a human health point of view. In this study, AuNPs@PMo_{12}, as a nanozyme, has been developed for the highly sensitive and selective detection of AP with 3,3′,5,5′-tetramethylbenzidine (TMB) within a few seconds without adding oxidizing reagents (*e.g.* H_2O_2). Synthesized nanosensors are able to oxidize TMB to yellow-brown oxidized TMB (oxTMB). The maximum peak wavelength of oxTMB was observed at 450 nm. The addition of AP and then increasing its concentration led to the production of different products in blue color. In experimental measurements, the limit of detection was obtained as 14.52 mg L^{-1}. The quantitative determination of AP concentrations can be carried out using UV-vis spectroscopy. The design of nanosensors is cost-effective and application of them in H_2O_2-free and enzyme-free conditions provides a rapid sensing approach for practical use in disease monitoring and diagnosis.

Received 28th July 2020
Accepted 18th September 2020

DOI: 10.1039/d0ra06545e

rsc.li/rsc-advances

Introduction

Colorimetric sensing using nanomaterials provides a competitive approach in point-of-care sensing owing to not using enzymes.[1,2] One of the best candidates for colorimetric detection is gold nanoparticles (AuNPs), due to their surface plasmon resonance which depends on distance.[3,4] Recently, the development of enzyme mimetic nanostructured materials has been a matter of great concern.[5,6] Using nanomaterials as enzymes (*i.e.* nanozymes) in comparison with natural enzymes shows many advantages such as cost-effective, easy and green production, high stability, and robustness. However, metal-based nanomaterials exhibit enzyme-like activities and have been used in immunoassay applications and biosensing.[7,8] It is important to notice that the enzyme-like activities of nanozymes depend on the manipulation of some properties, including size, shape, composition, and surface modification.[9] It is reported that surface modifications can be more prevailing due to catalytic reactions that occur on the surfaces of nanozymes. 3,3′,5,5′-Tetramethylbenzidine (TMB) is a green noncarcinogenic chromogenic material for colorimetric sensing,[19,20] normally applied as a noncarcinogenic colour reagent in enzyme-linked immunosorbent assays (ELISA).[10]

According to the literature, AuNPs show high activities in catalytic oxidation of TMB in the presence of hydrogen peroxide.[10] Ni *et al.*[11] developed a technique to detect melamine according to the peroxidase-like activity of gold nanoparticles.[11] Wang *et al.*[12] proposed the peroxidase-like activity of AuNPs and the effect of surface modification. They showed that bare AuNPs exhibit higher peroxidase activity in comparison to amino or citrate modified gold nanoparticles. It was also found that the surface charge of nanoparticles and substrates could be an important parameter in the catalytic activity.[12] Jv *et al.* reported that cysteamine-modified positively charged gold nanoparticles and citrate-capped negatively charged gold nanoparticles have different peroxidase-like activities.[13] They found that the surface charge of gold nanoparticles plays a crucial role in their catalytic activity.

Polyoxometalates (POMs) have received great interest owing to their wide range of applications in biochemistry, catalyst,[14] and sensing.[15] POMs can be used as reducing and stabilizing agents in aqueous solutions in ambient conditions.[16,17] Also, POMs can be used as a multi-electron reducing agent which is useful for the preparation of noble metal nanoparticles.[18,19]

According to the literature, POMs can be used as a catalyst for H_2O_2-based oxidation of organic materials in the presence of O_2 and H_2O_2 *via* multistep electron-transfer processes.[20–22] Thus, POMs can be applied as enzyme mimics to catalyse H_2O_2-based oxidation of 3,3′,5,5′-tetramethylbenzidine (TMB).[23] Li *et al.* prepared three tetra-nuclear ZrIV-substituted POMs, which exhibit peroxidase-like activities.[24] It was found that most of the POMs are stable and have more enzyme activities at low pH values (about 3.0 or 4.0).[23,24] However, it is interesting to develop

[a]*Department of Chemical Engineering, Quchan University of Technology, Quchan 94771-67335, Iran. E-mail: t.rohani@qiet.ac.ir; tahereh.rohani@gmail.com*

[b]*Department of Chemical Engineering, Quchan University of Technology, Quchan 94771-67335, Iran*

† Electronic supplementary information (ESI) available. See DOI: 10.1039/d0ra06545e

intrinsic oxidase nanozymes since they do not use harmful H_2O_2 as a co-substrate.

Acetaminophen (AP) is normally used as a medicine in the world.[25] The toxic dose of AP leads to acute liver injuries and liver failures.[26] The majority of acute liver failures are because of acetaminophen overdose, so it is vital to design a method with rapid quantitative detection of AP in emergency rooms. The most recent techniques for the detection of AP are a variety of analytical approaches like titrimetric methods,[27] high-performance liquid chromatography (HPLC),[28] spectrophotometry,[29] chemiluminescence,[30] and electrochemical analysis.[31] Colorimetric sensing of analytes is one of the techniques which provide personalized and clinical point-of-care (POC) diagnosis.

In the present research, a nanozyme, polyoxometalate-stabilized gold nanoparticles (AuNPs@PMo_{12}) was prepared under ultrasonic irradiation according to the previous literature.[32] Sono-synthesized samples were kept at room temperature and remained stable for more than three months. The as-prepared nanosensor showed remarkable oxidase-like activity of colourless TMB into the coloured product in the free H_2O_2 medium. The synthesized nanosensor was used for the naked-eye detection and showed a highly selective and specific determination of AP. The obtained results confirmed that the colorimetric reaction between AuNPs–PMo_{12} as a nanoprobe takes place within a few seconds. The color of the AuNPs@PMo_{12} nanohybrid solution changed a few seconds after mixing with TMB solution which confirms the rapid sensing of synthesized nanozyme. Moreover, it was found that the oxidase-like activity of AuNPs@PMo_{12} was improved in the presence of ionic species like PMo_{12} and Au^{3+}, $[AuCl_4]^-$. Synthesized nanosensors could oxidize TMB to (oxTMB) and induced a yellow-brown colour solution corresponding to an absorption peak centered at 450 nm. The addition of AP and increasing its concentration led to the production of blue products. In experimental measurements, the limit of detection was obtained 14.52 μg mL^{-1}. The quantitative determination of AP concentrations can be carried out using UV-vis spectroscopy. To achieve the optimized value of AuNPs@PMo_{12} nano-hybrids for sensing application, reaction temperature, and sample pH were investigated. The design of nanosensor is cost-effective and is operated in H_2O_2-free and enzyme-free conditions, which provide a new avenue for rapid sensing in disease monitoring and diagnosis.

Experimental

Materials

All reagents were obtained and used without further purification. Phosphomolybdic acid ($H_3PMo_{12}O_{40}$) (PMo_{12}), sodium hydroxide, and hydrochloric acid (37%) were purchased from Merck Company. 1-Propanol (C_3H_7OH) and 3,3′,5,5′-tetramethylbenzidine (TMB) were commercially available from Sigma-Aldrich. $HAuCl_4$ solution (0.1 M, 3.4% w/v) was freshly purchased from Kimia Next Company, Iran. Acetaminophen ($C_8H_9NO_2$), methadone ($C_{21}H_{27}NO$), methylphenidate ($C_{14}H_{19}NO_2$), aspirin ($C_9H_8O_4$), and tramadol ($C_{16}H_{25}NO_2$) were obtained from Temad Pharmaceutical Company in Iran. The physicochemical properties of AP are illustrated in Table S1.†[33] Milli-Q water was used with minimum resistivity of 18.2 MΩ cm^{-1}.

Sonochemical preparation of AuNPs@PMo_{12}

Sonochemical preparation of AuNPs@PMo_{12} carried out by high power sonicator (20 kHz) at three different temperatures (27 ± 1 °C, 37 ± 1 °C, and 47 ± 1 °C) for 30 minutes with Au : POM ratio of 1 : 2 and acoustic amplitude of 50%. The as-prepared products were used for the characterization analysis and detection of AP. The synthesis pathway was according to the previous study.[32] Briefly, the $HAuCl_4$ solution (1 mM, 16.5 mL) and PMo_{12} (1 mM, 33 mL) were mixed and stirred at room temperature. After that, the resulting solution was transferred into 100 mL Dewar cell, and 1.2 mL of propanol was added into this solution. The final solution was exposed to ultrasonic irradiation through an ultrasonic horn (20 kHz, Branson Digital Sonifier-USA, and W-450 D). The acoustic amplitude of the sonicator was adjusted on 50%, which delivered acoustic power of 25 W. The obtained reaction medium turned into wine red, showing the production of gold nanoparticles. Finally, the as-prepared AuNPs@PMo_{12} solution was kept at room temperature and remained stable for more than three months.

Detection of acetaminophen (AP) by UV-vis spectrum measurements

AuNPs@PMo_{12} nanohybrid was used for the colorimetric detection of AP. 0.9 mL of an AP aqueous solution with different concentrations (0–120 mg L^{-1}) were mixed separately with 0.9 mL of AuNPs@PMo_{12} solution and 0.1 mL of TMB solution (0.7 mM in ethanol). After that, the color change of the solution was monitored by UV-visible spectroscopy. Control solutions containing 0.1 mL of TMB (0.7 mM in ethanol), 0.9 mL of AuNPs@PMo_{12} solution and 0.9 mL of Milli-Q-water were prepared.

Characterization and apparatus

To obtain the crystal structure of nanohybrids, Bruker D8-Focus with Cu Kα radiation ($\lambda = 0.154056$ nm) was used in the range of 2θ = 10–80°. High-angle annular dark field-scanning transmission electron microscopy (HAADF-STEM) images were taken with TecnaiS-Twin 30, 300 keV, GIF-TRIDIEM. Energy-dispersive X-ray spectroscopy (EDS) data were measured using the same instrument. The UV-vis spectra were performed using an Evolution 201 Spectrophotometer (Thermo Fisher Scientific). IR spectra were recorded on a Thermo Nicolet Avatar-370-FTIR Spectrometer (Thermo Fisher Scientific, United States). Zeta-potential measurement was carried out using Zeta Compact (CAD Instrumentation, France). Dynamic Light Scattering (DLS) was conducted on Vasco Particle Size Analyzer (Cordouan Technologies). The electrochemical analysis was conducted using a μ-Autolab type III electrochemical workstation. The analysis was done at room temperature using a conventional three-electrode set-up. Platinum wire (Azar Electrode Co.) served as the counter electrode and Ag/AgCl as the reference

electrode (Azar Electrode Co.). The sonochemical procedure was conducted using equipment operating at 20 kHz (Branson Digital Sonifier, Model W-450 D). It includes a double cylindrical jacket with a volume of 100 mL to control the temperature. The 20 kHz ultrasonic irradiations were emitted from the tip with a diameter of 1.1 cm which was located at the end of the horn.

Determination of acoustic intensity

Acoustic power and intensity were determined by the colorimetric method.[34] In this work, an amplitude of 50% was used to deliver acoustic power of 25 W and an intensity of 26 W cm^{-2}.

Results and discussions

After the reduction of Au^{3+} ions with PMo_{12} as a stabilizing and reducing agents, the AuNPs@PMo_{12} nano-hybrids were characterized by UV-visible, FT-IR, HAADF-STEM, EDS, zeta potential, cyclic voltammograms (CVs), and DLS, respectively. The details of the reaction mechanism are presented in ESI.† The characterization of AuNPs@PMo_{12} nano-hybrids is also discussed in ESI.†

Design of the proposed colorimetric sensor

The colorimetric analytical technique has attracted considerable attention due to some advantages such as simplicity, cost-effectiveness, and no need of any complicated or expensive instruments. TMB is commonly used as a chromogenic substrate, especially in enzyme-linked immunosorbent assay (ELISA). TMB oxidation by catalyst or enzyme/enzyme-like in the presence of H_2O_2 generates a blue color, with absorbance peaks at 370 and 652 nm.[35] There are some limitations, in terms of reaction conditions, on biological detection. Besides, the enzymatic reaction requires strict conditions, such as pH control, catalyst type, and temperature control of the reaction.

As reported elsewhere, gold nanoparticles can oxidize 3,3′,5,5′-tetramethylbenzidine (TMB) in the presence of hydrogen peroxide to form a blue product.[12] TMB includes two amino groups, which show affinity to the surface of nanoparticle with a negative charge.[36] Besides, in acidic media (pH of 3.0 or 4.0), POMs show both higher enzyme activity and stability. But, the POM nanozymes become catalytically inactive in the physiological solutions (pH 7.0–7.5). The enzyme-like activities of POMs with Keggin type structures were reported.[23] It was claimed that Mo and W as coordination atoms show more influence on the enzyme-like activity of POM.[23] According to another literature, polyoxomolybdates ($H_3PMo_{12}O_{40}$) can oxidize TMB as a substrate to form a blue color substance with maximum absorbance at 650 nm and without the presence of H_2O_2.[23]

So, we choose AuNPs decorated with PMo_{12} to oxidize TMB due to more stability of AuNPs than enzymes. Here, the catalytic activity of AuNPs@PMo_{12} on the colorimetric reaction of TMB in the absence of H_2O_2 was investigated. Also according to another literature, unreacted Au^{3+} ions and PMo_{12} which exist in the AuNPs@PMo_{12} solution could help to oxidize TMB to oxTMB.[12]

Mechanism investigation on colorimetric sensing of AP

As stated in the literature, TMB can be oxidized into its free cationic radical form *via* single electron transfer.[37] Furthermore, different TMB derivatives in the reaction medium can be generated like charge-transfer complex and di-imine (di-cation due to double electron transfer).[37] The charge-transfer complex is blue, with absorbance peaks at 652 and 370 nm and two-electron oxidation, di-imine derivative (450 nm) with yellow color (Fig. S2†).[37]

In our study, with the addition of as-prepared AuNPs@PMo_{12} solution, the colorless solution of TMB changed into yellow-brown, and a maximum absorbance at 450 nm was monitored (Fig. 1). These results indicate that TMB is oxidized directly into di-imine derivative by the AuNP@PMo_{12} solution in the absence of H_2O_2.

When the AP solution was added and its concentration increased, the yellow-brown color oxTMB transformed into a dark orange-brown and finally into blue. As shown in Fig. 1, by the addition of AP solution with a concentration of 20 mg L^{-1}, two peaks were observed (460 and 600 nm) due to the presence of two forms of oxTMB in the solution (di-imine and charge-transfer complex). Increasing the concentration of AP to 30 mg L^{-1} led to the appearance of a peak at 610 nm and the absorbance peak of 460 nm diminished, which was due to the presence of one form of oxTMB (di-imine structures).

To prove the mechanism of the reaction, the effects of reagents, including $HAuCl_4$, PMo_{12}, precursor solution, and pure AuNPs@PMo_{12} on oxidation of TMB were separately investigated. In all cases, the color change was monitored a few seconds after mixing with TMB solution.

In the case of $HAuCl_4$ solution, a few seconds after mixing TMB and $HAuCl_4$ solution, the color of the solution changed into yellow (Fig. 2). The absorption peak at 450 nm appeared due to the formation of oxidized tetramethylbenzidine, diimine derivative (450 nm), which showed that $HAuCl_4$ can directly oxidize TMB into the di-imine derivative. Generally, different

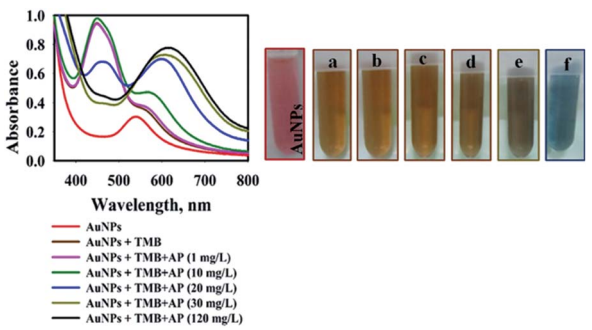

Fig. 1 UV-Vis spectra of AuNPs@PMo_{12} in presence of TMB solution with different concentration of AP, photographic images: (a) AuNPs + TMB, (b) AuNPs + TMB + AP (1 mg L^{-1}), (c) AuNPs + TMB + AP (10 mg L^{-1}), (d) AuNPs + TMB + AP (20 mg L^{-1}), (e) AuNPs + TMB + AP (30 mg L^{-1}), (f) AuNPs + TMB + AP (120 mg L^{-1}).

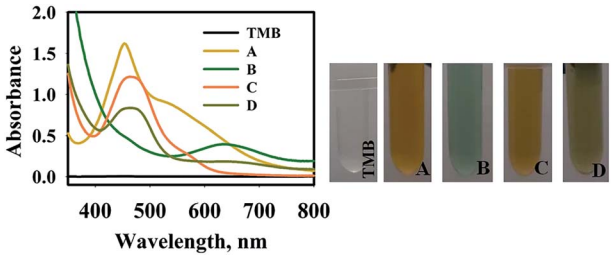

Fig. 2 UV-Vis spectra of TMB solution, (A) TMB–Au(III) ($HAuCl_4$(III)) (0.9 mL, 1 mM) + Milli-Q water (0.9 mL) + TMB solution 0.1 mL, 0.7 mM), (B) TMB–PMo_{12} (PMo_{12} (0.9 mL, 1 mM)+ Milli-Q water (0.9 mL) + TMB solution 0.1 mL, 0.7 mM), (C) TMB–precursor solution (precursor solution (0.9 mL) + Milli-Q water (0.9 mL) + TMB solution 0.1 mL, 0.7 mM), (D) TMB–precursor solution (precursor solution (0.9 mL) + AP (0.9 mL, 100 mg L^{-1}) + TMB solution 0.1 mL, 0.7 mM).

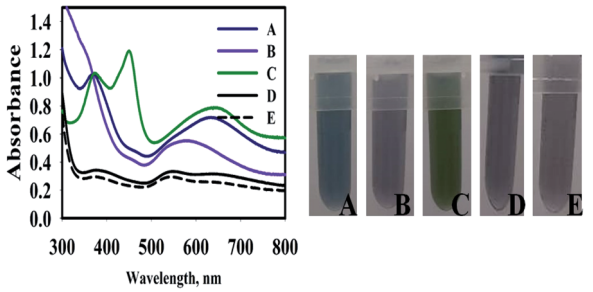

Fig. 3 UV-Vis spectra of (A) AuNPs@PMo_{12} (0.9 mL) + $HAuCl_4$ (0.05 mL, 1 mM) + PMo_{12} (0.05 mL, 1 mM) + AP (30 mg L^{-1}, 0.9 mL) + TMB solution (0.1 mL, 0.7 mM), (B) AuNPs@PMo_{12} (0.9 mL) + PMo_{12} (0.1 mL, 1 mM) + AP (30 mg L^{-1}, 0.9 mL) + TMB solution (0.1 mL, 0.7 mM), (C) AuNPs@PMo_{12} (0.9 mL) + $HAuCl_4$ (0.1 mL, 1 mM) + AP (30 mg L^{-1}, 0.9 mL) + TMB solution (0.1 mL, 0.7 mM), (D) AuNPs@PMo_{12} (0.9 mL) + Milli-Q-water (0.9 mL) + TMB solution (0.1 mL, 0.7 mM), (E) AuNPs@PMo_{12} (0.9 mL) + AP (30 mg L^{-1}, 0.9 mL) + TMB solution (0.1 mL, 0.7 mM).

specious of gold ions can be produced in an aqueous solution such as Au^{+}, Au^{3+}, and anionic-chloro complex $[HAuCl_4]^{-}$.[38] It is proposed that Au^{3+} ions tend to withdraw electrons from TMB structure which leads to double electron transfer and production of the di-imine derivative.

As shown in Fig. 2, the absorption spectrum of TMB–PMo_{12} solution with an absorption peak at 640 nm was observed. Light green is assigned to the charge-transfer complex, which confirms the oxidation of TMB in presence of PMo_{12} in acidic medium. This observation confirms other literature results about the oxidization of TMB into blue color using polyoxomolybdates in the absence of H_2O_2.[23]

The addition of TMB into precursor solution in the absence and presence of AP (100 mg L^{-1}) was conducted, appearing a yellow and olivaceous color with an absorption peak at 470 nm. These results suggest the direct oxidation of TMB into the di-imine derivative. It was observed that the intensity of the absorption peak of the TMB solution in the presence of AP drastically decreased compared to the absence of AP. It is proposed that the Au(III) ions which interacted with the –OH group of AP ($C_8H_9NO_2$) molecules *via* donor–acceptor electron complex[32] can reduce the catalytic activity of Au(III) on oxidation of TMB molecules. Besides, the electrostatic attraction of negatively charged anionic species including $[AuCl_4]^{-}$ and PMo_{12} to the amine group of TMB could help to oxidize the TMB. By adding AP solution, anionic species interacted with the amine group of AP and reduced the interaction with TMB molecules.

To investigate the mechanism of TMB oxidation in the presence of nanosensors, the final product was centrifuged and washed many times, in order to purify and separate it from the synthesis media. The purified AuNPs@PMo_{12} was dispersed in deionized water and tested with TMB solution in the presence and absence of an AP solution. According to the results (Fig. 3), no oxidase-like activity of the pure Au NPs was observed in the presence and absence of AP molecules. While, after the addition of $HAuCl_4$ and PMo_{12} into the AuNPs solution in the presence of AP (100 mg L^{-1}), the color of TMB changed to blue with observed peaks at 640 nm and 370 nm due to oxidation of TMB into charge-transfer complex. To investigate the effect of PMo_{12} and $HAuCl_4$ separately, each of them was added in purified AuNPs in the presence of AP (100 mg L^{-1}). As shown in Fig. 3, the addition of PMo_{12} led to a change of color into dark purple and a shift of absorption peak to 570 nm. The addition of $HAuCl_4$ led to the appearance of three absorption peaks at 370, 450, and 652 nm on the absorption spectrum of TMB–Au(III) solution. These wavelengths (370 nm and 652 nm) are assigned to charge-transfer complex of oxidized tetramethylbenzidine and di-imine derivative (450 nm). It is concluded that the presence of $HAuCl_4$ shows a predominant role in the oxidation of TMB. The significant performance of $HAuCl_4$ is due to its ionic species including Au^{3+} and $[AuCl_4]^{-}$. Therefore, the synergic effect of $HAuCl_4$, PMo_{12}, and AuNPs on oxidation of TMB in the presence of AP molecules was confirmed.

It this research, the synergic effect of PMo_{12}, $AuCl_4^{-}$, and AuNPs@PMo_{12} under acidic conditions (pH of nanosensor) led to direct oxidation of TMB into a di-imine derivative ($\lambda = 450$ nm) with yellow-brown color. With the addition of AP solution and consequently increasing its concentration, oxidized tetramethylbenzidine, di-imine derivative changed to a charge-transfer complex product and caused a color change.[37]

The brown solution turned into blue and the absorbance at 450 nm was slowly decreased, exhibiting a typical reaction product absorption at 610 nm. According to previous research, AuNPs@PMo_{12} nanohybrid is aggregated in the presence of Au(III) and AP.[32] As seen in Fig. 4, by adding AP into AuNPs@PMo_{12} solution some islands of AuNPs aggregates were seen. As mentioned in the previous study, Au(III) ions interacted with the –OH group of AP ($C_8H_9NO_2$) molecules *via* donor–acceptor electron complex.[32] Besides, AP molecules with a functional group (–NH) form a hydrogen bonding and donor–acceptor electron complexes into the AuNPs@PMo_{12} surface. Therefore, AP molecules in the presence of Au(III) can induce the AuNPs@PMo_{12} aggregation.[32] Thus, fewer amounts of active sites for the oxidation of TMB were accessible and the complete oxidation of TMB was prevented.

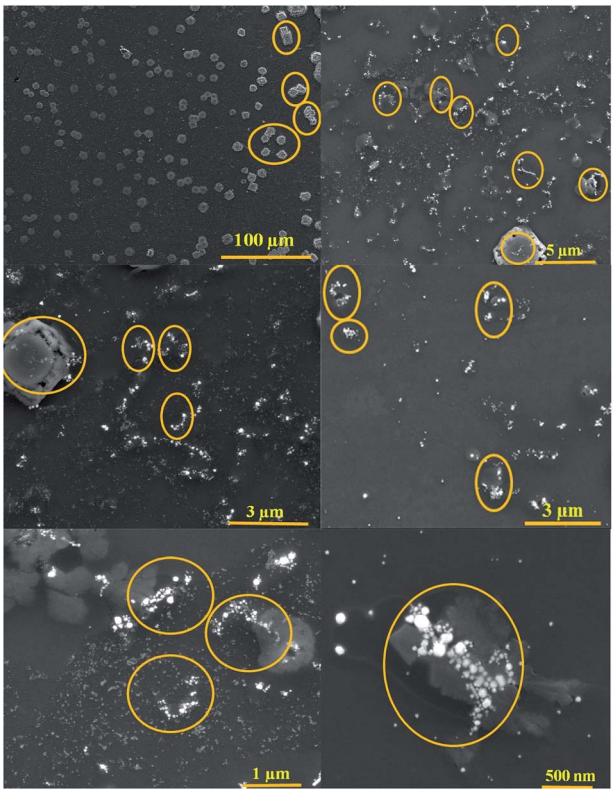

Fig. 4 SEM images of AuNPs@PMo_{12} nano-hybrids after the addition of AP (70 mg L^{-1}) (marked area shows aggregated particles).

To prove the aggregation of AuNPs@PMo_{12} nanohybrids after the addition of AP (150 mg L^{-1}) and TMB, DLS analysis was performed to measure the size distribution and hydrodynamic diameter of AuNPs@PMo_{12}. The average size of AuNPs@PMo_{12} increased from 19.8 ± 1.7 nm to 42.17 ± 3.92 nm after the addition of AP (150 mg L^{-1}) which confirmed the proposed mechanism about the aggregation AuNPs in presence of AP molecules. After adding TMB solution the size of AuNPs more increased to 72.41 ± 1.5 nm (Fig. S3†). It is suggested that Au^+ ions reduced to Au in presence of TMB molecules according to the following equation:

$$Au^+ + TMB \rightarrow Au + TMB^+ \quad (1)$$

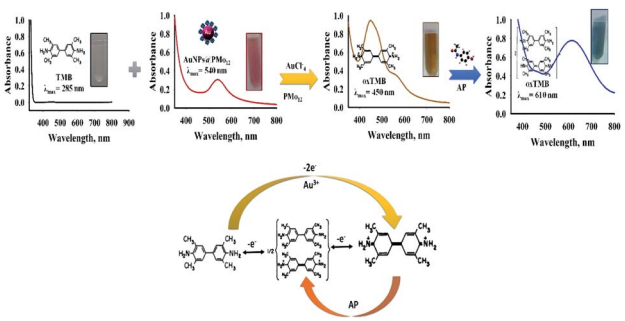

Scheme 1 Oxidation pathway of 3,3′,5,5′-tetramethylbenzidine (TMB) using AuNPs@PMo_{12}.

Scheme 1, illustrates the oxidation pathway of 3,3′,5,5′-tetramethylbenzidine (TMB) using AuNPs@PMo_{12} in the presence of Au ionic species and unreacted PMo_{12}.

Optimization studies for acetaminophen detection

The sensing conditions such as reaction temperature and sample pH on AP sensing were further optimized.

The effect of temperature was investigated at 27 ± 1 °C, 37 ± 1 °C, and 47 ± 1 °C (Fig. 5). To investigate the effect of reaction temperature, AP aqueous solution (0.9 mL) was added to the AuNPs@PMo_{12} solution (0.9 mL) and TMB solution (0.1 mL + 0.7 mM). After a few seconds, the color of the solution changed from yellow-brown (AP, 0 mg L^{-1}) to blue (AP, 30 mg L^{-1}).

As Fig. 5, the addition of AP into nanosensor solution, which was prepared in 37 ± 1 °C in the presence of TMB, led to a more significant SPR peak at 610 nm and a dark blue color. In the case of nanosensor which was synthesized at 27 ± 1 °C and 47 ± 1 °C, two peaks were observed (460 and 610 nm) due to the presence of two forms of oxTMB in solution. At higher temperatures, the UV-vis spectrum shows a significant sharp peak at 450 nm, which confirms the presence of di-imine structure as a predominant form of oxTMB in the solution.

It is assumed that in higher temperatures, fewer amounts of unreacted Au(III) ions leave in the solution due to the higher rate of reaction. So, fewer amounts of AuNPs were aggregated[32] and AuNPs could completely oxidize TMB molecules to di-imine structures. In our case, as the monitoring of the blue color (λ_{max}= 620 nm) was evident for quantitatively detection of AP, the temperature of 37 ± 1 °C was selected as the optimum temperature.

The second parameter which was optimized was the influence of sample pH on oxidation of TMB solution in the presence of AuNPs@PMo_{12} nanosensor. The pH of the AuNPs@PMo_{12} solution was 3.0 ± 0.5, and the other pH values were adjusted using NaOH solution. According to Fig. 6, the strong oxidation of TMB and the formation of dark blue color occurred at lower pH and acidic media. Also, increasing the pH of the solution led to fewer amounts of oxTMB forms.

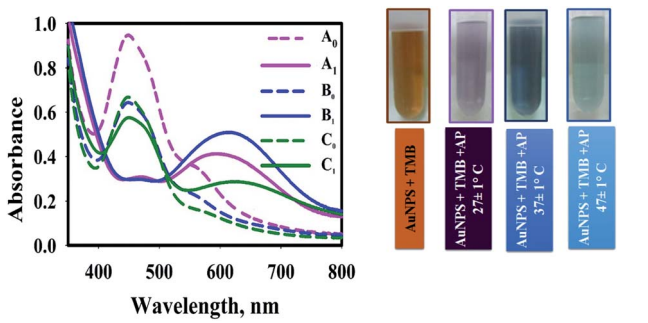

Fig. 5 Effect of reaction temperature on SPR peak of AuNPs@PMo_{12} upon addition of AP (A_0: AuNPs + TMB, A_1: AuNPs + TMB + AP (30 mg L^{-1}), *T*; 27 ± 1 °C, B_0: AuNPs + TMB, B_1: AuNPs + TMB + AP (30 mg L^{-1}), *T*; 37 ± 1 °C, C_0: AuNPs + TMB, *T*; C_1: AuNPs + TMB + AP (30 mg L^{-1}), 47 ± 1 °C) (pictures show visual color change due to addition of AP solution into AuNPs@PMo_{12} solution in presence of TMB).

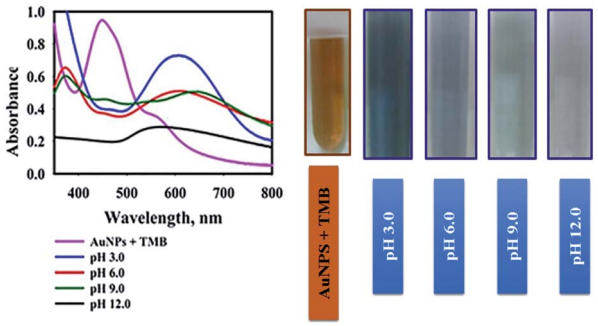

Fig. 6 Effect of pH sample on SPR peak of AuNPs@PMo_{12} upon addition of AP (30 mg L^{-1}) at different pH in presence of TMB, pictures show visual color change due to addition of AP solution into AuNPs@PMo_{12} solution in presence of TMB.

According to the literature, in acidic media (about pH value 3 or 4), POMs are more stable and show more enzyme activities. Furthermore, at higher pH (pH $\geq$ 7.0–7.5), the POM nanozymes are catalytically inactive.[23]

Also in the basic media, PMo_{12} is not stable; therefore, it may be degraded to some new Mo-based compounds and change the structure of the nano-hybrid. Consequently, pH 3.0 $\pm$ 0.5 (natural pH of nanosensor) was selected for AuNPs@PMo_{12}-based colorimetric assays of AP.[32]

Determination of AP on the proposed colorimetric sensor

The UV-vis absorption spectra of AP with different concentrations in the presence of AuNPs@PMo_{12} and TMB solution were recorded (Fig. 7). According to Fig. 7, the color turned from yellow-brown to orange-brown and then into blue by increasing the AP solution.

As shown in Fig. 7, by increasing AP concentration, the absorbance of the TMB media at 450 nm significantly decreased. The absorption values also showed a good linear correlation with the concentration of AP in the range of 30–120 mg L^{-1} with a regression equation of $y = 0.0007x + 0.704$ (0.99) shown in Fig. 6b. Based on $3\sigma/s$, where σ is the standard deviation of the blank measurements and s is the sensitivity of the calibration graph, the detection limit of AP was calculated to be 14.52 μg mL^{-1}. It is important to notice that the toxic level of AP in human serum is more than 100 mg L^{-1}.[32]

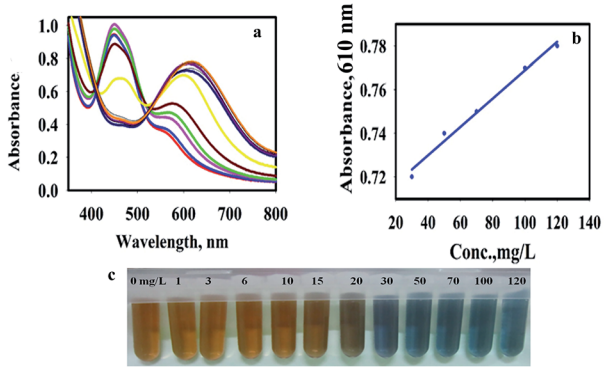

Fig. 7 (a) UV-visible spectra of AuNPs@PMo_{12} solutions with different concentrations of AP in presence TMB, (b) calibration graphs for the quantification of AP by using AuNPs@PMo_{12} as the colorimetric probe, and photographic images of AuNPs@PMo_{12} in the concentration range of 1 mg L^{-1} to 120 mg L^{-1} (concentrations of all AP solution were (from left to right) 0, 1, 3, 6, 10, 15, 20, 30, 50, 70, 100 and 120 mg L^{-1}, respectively).

Specificity for AP

The specificity of the AuNPs@PMo_{12} nano-hybrid was performed by comparing the color change of solution, including seven drugs (acetaminophen, methadone, methylphenidate, tramadol, ibuprofen, aspirin, and diclofenac) separately. In this test, acetaminophen,AP ($C_8H_9NO_2$), methadone, MTD ($C_{21}H_{27}NO$), methylphenidate, MEPS ($C_{14}H_{19}NO_2$), tramadol, TRA ($C_{16}H_{25}NO_2$), ibuprofen, IBP ($C_{13}H_{18}O_2$), aspirin, ASA ($C_9H_8O_4$), diclofenac, DIC ($C_{14}H_{11}Cl_2NO_2$) with a concentration of 0.4 mmol L^{-1} were added into AuNPs@PMo_{12} solution.

As seen in Fig. 8, an obvious change in color, from yellow-brown to blue, was immediately observed after adding AP, whereas the others were still yellow-brown. The characteristic color changes were further confirmed by UV-Vis spectrum and only the target of AP leads to an obvious red-shift effect into 610 nm. According to the previous result, only AP molecules can react onto the surface of AuNPs@PMo_{12}.[32] So, the color change into the blue was seen in the presence of AP molecules.

Kinetic studies of AuNPs@PMo_{12} nanohybrid

To understand the kinetic properties of AuNPs@PMo_{12} nanohybrid more precisely, steady-state kinetic assays were carried out in the presence of different concentrations of TMB. The

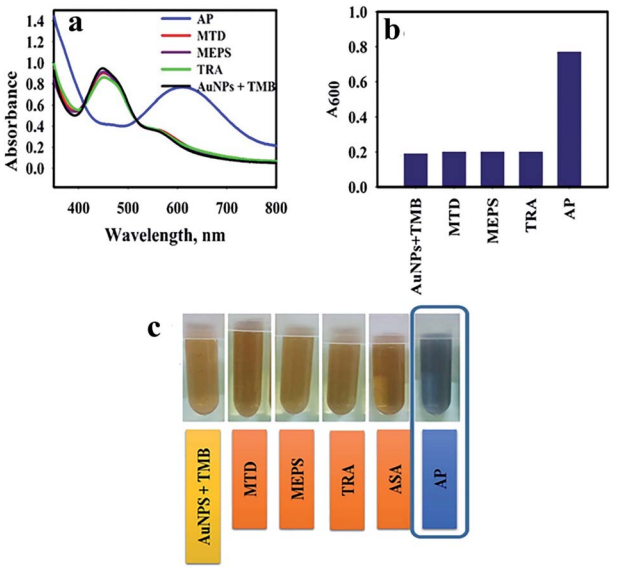

Fig. 8 (a) UV-visible spectra of AuNPs@PMo_{12} solutions with different drugs, (b) effect of the addition of different drugs on the absorbance 600 nm (A_{600} nm) of the AuNPs@PMo_{12} (concentration of all drugs, 0.4 mmol L^{-1}), and (c) photographic images of AuNPs@PMo_{12} nanohybrid aggregation with drugs.

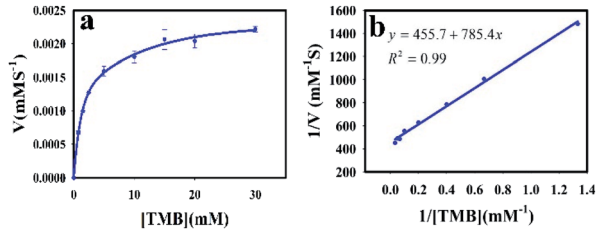

Fig. 9 The steady-state kinetic study of AuNPs@PMo_{12}; (a) TMB concentration varied between 0.75 and 30 mM (AP, 100 mg L^{-1}), (b) the corresponding Lineweaver–Burk plots of the Michaelis–Menten equation.

experiments were conducted according to the enzyme kinetics theory. The kinetics data at the varying substrate (TMB) was plotted to fit the Michaelis–Menten equation (2). As seen in Fig. 9, the typical Michaelis–Menten (Fig. 9a) and Lineweaver–Burk plots (eqn (3)) (Fig. 9b) were plotted at a given concentration range of TMB.

$$V_0 = \frac{V_m[S]}{K_m + [S]} \quad (2)$$

$$\frac{1}{V_0} = \frac{K_m}{V_m}\frac{1}{[S]} + \frac{1}{V_m} \quad (3)$$

where V_0 is the initial velocity (initial rate), [S] is the concentration of the substrate (TMB), K_m is the Michaelis–Menten constant and V_m is the maximal reaction velocity.

The enzymatic kinetic parameters like Michaelis–Menten constant (K_m) and the maximum reaction velocity (V_{max}) were determined by fitting the Lineweaver–Burk equation. K_m is a kinetic parameter that identifies the enzyme affinity towards the substrates. The low value of K_m is related to the higher enzyme affinity to a substrate and *vice versa*.[39,40]

The K_m and V_m values of AuNPs@PMo_{12} for TMB have obtained 1.57 mM, and 2.2×10^{-3} mM s^{-1} which offer AuNPs@PMo_{12} as a suitable artificial enzyme.

Conclusions

In this research, for the first time, AuNPs@PMo_{12} as nanozyme was developed for the qualitative and quantitative determination AP based on TMB colorimetric nanosensor in H_2O_2-free conditions. The limit of detection reaches to 14.52 μg mL^{-1}. The proposed mechanism of AP detection using AuNPs@PMo_{12} as nanozyme for the oxidation of TMB in H_2O_2 free media is as follows: the synergic effects of $HAuCl_4$, PMo_{12}, and AuNPs@PMo_{12} were effective for oxidation of TMB in the absence of H_2O_2. The role of Au(III) ionic species was predominant. Furthermore, in the presence of AP molecules due to aggregation of AuNPs *via* Au(III) ions, less active sites were available for the oxidation of TMB. Thus, di-imine derivative changed to charge-transfer complex product.

The detection is quite simple in preparation and operation and can be completed within a few seconds. The developed strategy provides a cost-effective and efficient approach for potential applications in clinical diagnosis.

Conflicts of interest

The authors declare no conflict of interest.

Acknowledgements

This work has been financially supported by the Iranian National Science Foundation (INSF) (No. 97009286). The authors also wish to thank Dr Scott G. Mitchell from Zaragoza University for HAADF-STEM analysis.

References

1 H. H. Deng, X. L. Lin, Y. H. Liu, K. L. Li, Q. Q. Zhuang, H. P. Peng, A. L. Liu, X. H. Xia and W. Chen, *Nanoscale*, 2017, **9**, 10292–10300.
2 T. Wang, P. Su, F. Y. Lin and Y. Yang, *Sens. Actuators, B*, 2017, **254**, 329–336.
3 K. Hobbs, N. Cathcart and V. Kitaev, *Chem. Commun.*, 2016, **52**, 9785–9788.
4 G. Sener, L. Uzun and A. Denizli, *ACS Appl. Mater. Interfaces*, 2014, **6**, 18395–18400.
5 Y. Huang, J. Ren and X. Qu, *Chem. Rev.*, 2019, **119**, 4357–4412.
6 J. Wu, X. Wang, Q. Wang, Z. Lou, S. Li, Y. Zhu and H. Wei, *Chem. Soc. Rev.*, 2019, **48**, 1004–1076.
7 Q. Wang, H. Wei, Z. Zhang, E. Wang and S. Dong, *TrAC, Trends Anal. Chem.*, 2018, **105**, 218–224.
8 K. Korschelt, M. N. Tahir and W. Tremel, *Chem.–Eur. J.*, 2018, **24**, 9703–9713.
9 C. Liu, K. Chen, C. Su, P. Yu and P. Lee, *Catalysts*, 2019, **9**, 517.
10 Z. Xue, L. Xiong, H. Rao, X. Liu and X. Lu, *Dyes Pigm.*, 2019, **160**, 151–158.
11 P. Ni, H. Dai, Y. Wang, Y. Sun, Y. Shi, J. Hu and Z. Li, *Biosens. Bioelectron.*, 2014, **60**, 286–291.
12 S. Wang, W. Chen, A. Liu, L. Hong, H. Deng and X. Lin, *ChemPhysChem*, 2012, **13**, 1199–1204.
13 Y. Jv, B. Li and R. Cao, *Chem. Commun.*, 2010, **46**, 8017–8019.
14 H. G. T. Ly, G. Absillis, R. Janssens, P. Proost and T. N. Parac-Vogt, *Angew. Chem., Int. Ed.*, 2015, **54**, 7391–7394.
15 A. González, N. Gálvez, M. Clemente-León and J. M. Dominguez-Vera, *Chem. Commun.*, 2015, **51**, 10119–10122.
16 D.-F. Chai, Z. Ma, H. Yan, Y. Qiu, H. Liu, H.-D. Guo and G.-G. Gao, *RSC Adv.*, 2015, **5**, 78771–78779.
17 L. Suo, W. Gao, Y. Du, R. Wang, L. Wu and L. Bi, *New J. Chem.*, 2016, **40**, 985–993.
18 G. Zhang, B. Keita, R. N. Biboum, F. Miserque, P. Berthet, A. Dolbecq, P. Mialane, L. Catala and L. Nadjo, *J. Mater. Chem.*, 2009, **19**, 8639–8644.
19 R. Liu, S. Li, G. Zhang, A. Dolbecq, P. Mialane and B. Keita, *J. Cluster Sci.*, 2014, **25**, 711–740.
20 D. L. Long, R. Tsunashima and L. Cronin, *Angew. Chem.*, 2010, **122**, 1780–1803.
21 N. Mizuno, K. Yamaguchi and K. Kamata, *Coord. Chem. Rev.*, 2005, **249**, 1944–1956.

22 S. Liu, *et al.*, *ChemPlusChem*, 2012, **77**, 541–544.
23 B. Zhang, M. Zhao, Y. Qi, R. Tian, B. Carter, H. Zou, C. Zhang and C. Wang, *Sci. Rep.*, 2019, **9**, 14832.
24 D. Li, *et al.*, *Chem.–Eur. J*, 2013, **24**, 1926–1934.
25 E. Yoon, A. Babar, M. Choudhary, M. Kutner and N. Pyrsopoulos, *J. Clin. Transl. Hepatol.*, 2016, **4**, 131–142.
26 R. Clark, J. E. Fisher, I. S. Sketris and G. M. Johnston, *BMC Clin. Pharmacol.*, 2012, **12**, 11.
27 G. Burgot, F. Auffret and J.-L. Burgot, *Anal. Chim. Acta*, 1997, **343**, 125–128.
28 S. Ravisankar, M. Vasudevan, M. Gandhimathi and B. Suresh, *Talanta*, 1998, **46**, 1577–1581.
29 A. B. Moreira, H. P. Oliveira, T. D. Atvars, I. L. Dias, G. O. Neto, E. A. Zagatto and L. T. Kubota, *Anal. Chim. Acta*, 2005, **539**, 257–261.
30 S. Zhao, W. Bai, H. Yuan and D. Xiao, *Anal. Chim. Acta*, 2006, **559**, 195–199.
31 A. Cernat, M. Tertiș, R. Săndulescu, F. Bedioui, A. Cristea and C. Cristea, *Anal. Chim. Acta*, 2015, **886**, 16–28.
32 T. Rohani Bastami, A. Ghaedi, S. Mitchell, A. Javadian-Sarafe and M. Karimi, *RSC Adv.*, 2020, **10**, 16805–16816.
33 V. Bernal, A. Erto, L. Giraldo and J. C. Moreno-Piraján, *Molecules*, 2017, **22**, 1032.
34 T. Rohani Bastami and M. H. Entezari, *Ultrason. Sonochem.*, 2012, **19**, 560–569.
35 P. Ni, Y. Sun, H. Dai, J. Hu, S. Jiang, Y. Wang, *et al.*, *Biosens. Bioelectron.*, 2015, **63**, 47–52.
36 F. Yu, Y. Huang, A. J. Cole and V. C. Yang, *Biomaterials*, 2009, **30**, 4716–4722.
37 P. Josephygg, T. Elingg and R. Mason, *J. Biol. Chem.*, 1982, **257**, 3669–3675.
38 I. V. Mironov and E. V. Makotchenko, *J. Solution Chem.*, 2009, **38**, 725–737.
39 S. Mvango and P. Mashazi, *Mater. Sci. Eng., C*, 2019, **96**, 814–823.
40 S. Rostamia, A. Mehdiniab and A. Jabbari, *Mater. Sci. Eng., C*, 2020, **114**, 111034.